

# Exciton-LO-phonon dynamics in InAs/GaAs quantum dots: effects of zone-edge phonon damping

Paweł Machnikowski<sup>1,2</sup> and Lucjan Jacak<sup>1</sup>

<sup>1</sup>*Institute of Physics, Wrocław University of Technology, 50-370 Wrocław, Poland*

<sup>2</sup>*Institute für Festkörpertheorie, Universität Münster, 48149 Münster, Germany*

The dynamics of an exciton-LO-phonon system after an ultrafast optical excitation in an InAs/GaAs quantum dot is studied theoretically. Influence of anharmonic phonon damping and its interplay with the phonon dispersion is analyzed. The signatures of the zone-edge decay process in the absorption spectrum and time evolution are highlighted, providing a possible way of experimental investigation on phonon anharmonicity effects.

PACS numbers: 78.67.Hc,63.20.Kr

## I. INTRODUCTION

Unlike natural atoms, semiconductor quantum dots (QDs) always form part of a macroscopic crystal. The interaction with the quasi-continuum of lattice degrees of freedom (phonons) constitutes an inherent feature of these nanometer-size systems and cannot be neglected in any realistic modeling of QD properties, especially when the coherence of confined carriers is of importance. The understanding of the decisive role played by the carrier coupling to lattice modes has increased recently due to both experimental and theoretical study, including the effects of the carrier-phonon interaction in a system driven optically on ultrafast time scales<sup>1,2,3,4</sup>. The phonon-induced decoherence seems to be crucial for any quantum information processing application and for any nanotechnological device relying on quantum coherence of confined carriers<sup>5,6</sup>.

One of the issues of interest is the evolution of the carrier-lattice system after ultrafast excitation of carriers. Experiments performed on bulk and quantum well systems<sup>7,8,9,10,11</sup> show strongly non-Markovian behavior of carrier relaxation on 100 fs timescale due to pertinent system memory, yielding access to the quantum kinetic regime of the system dynamics where fundamental ideas of quantum mechanics may be tested.

For systems confined in all 3 dimensions, where purely longitudinal optical (LO) phonon relaxation is forbidden by energy conservation, coherent LO phonon dynamics may still be induced by lattice relaxation after non-adiabatic change of carrier distribution (dressing process<sup>4</sup>). In this process, an ultrafast excitation of confined carriers results in the lattice state which no longer corresponds to the energy minimum and therefore is unstable. Before the excess energy may be transferred outside the QD area (by radiating out phonons), a transient dynamics takes place, manifested by the oscillations (beats, overdamped for acoustical phonons) in the optical response of the system<sup>1</sup>.

Femtosecond time-resolved experiments showing the joint LO-phonon evolution (beats) in such quasi-0-dimensional systems were performed only on semiconductor nanocrystals<sup>12,13,14</sup>, where confined and surface

modes come into play, leading to different properties of the carrier-phonon coupling (e.g. size dependence<sup>15</sup>). For self-assembled semiconductor QDs, only 1 ps timescale dynamics was reported<sup>1</sup>. However, some theoretical models, developed for the description of nonlinear optical response in bulk or 2D systems<sup>16,17</sup>, may be successfully applied to the confined (0D) case with discrete carrier spectrum. Within such independent boson models it was possible to describe the linear<sup>2,18,19</sup> and nonlinear<sup>3</sup> response in the limit of infinitely short pulses and to account quantitatively<sup>3</sup> for the short-time behavior of optical polarization observed in the time-resolved spectroscopy experiment<sup>1</sup>. Although the observed effects may be attributed only to acoustic phonons<sup>3</sup>, the theory predicts also LO phonon effects for sufficiently short pulses<sup>2,15</sup>.

Due to the weak dispersion of LO modes effectively coupled to the confined carriers, the dephasing of LO phonon beats is extremely slow (100 ps timescale)<sup>4</sup>. On the other hand, anharmonic damping reduces the lifetime of a zone-center LO phonon in GaAs to 9.2 ps at low temperatures<sup>20</sup>. Hence, including the anharmonicity is essential for a correct description of the confined carrier-LO-phonon dynamics. The actual nature of anharmonic phonon-phonon interactions is, unfortunately, still unclear. Experimental results for the bulk GaAs<sup>20</sup> suggest dominant role of the decay channel to zone-edge LO and transversal acoustical (TA) phonons, although another interpretation of the same data proposes a major contribution of the decay into two longitudinal acoustical (LA) phonons<sup>21</sup>. The latter channel has been also studied theoretically both for bulk<sup>22</sup> and confined<sup>23</sup> LO phonons. Quite unexpectedly, phonon dispersion measurements<sup>24</sup> suggest that the zone-edge process may be forbidden by energy and momentum conservation. Since the anharmonic effects seem to be essential e.g. for correct modeling of relaxation phenomena<sup>15,25,26,27</sup>, this ambiguity is a real problem.

In the present paper we describe theoretically the quantum evolution of LO phonons damped by anharmonicity after an ultrafast carrier (exciton) excitation. We focus on the effects of the zone-edge decay process and its possible signatures in the spectral line shapes and

temporal dynamics. We single out various regimes both for single mode evolution and for the collective dynamics of all the coupled phonons. For each of these cases we calculate the linear optical absorption for frequencies corresponding to LO phonon peaks as well as the evolution of the reduced density matrix after an ultrafast excitation. Both characteristics (in frequency and time domain) are calculated within a single formalism, based on the Green function technique, restricted to single-phonon effects (which is a reasonable approximation in the weak coupling case at low temperatures) but incorporating the contribution from optically inactive exciton states excited by nonadiabaticity of LO phonon dynamics<sup>28</sup>. We show that the zone-edge decay of LO phonons manifests itself clearly in the spectral properties of the system for certain energy relations between the zone-center and zone-edge phonons. Although these energy relations are a material feature under fixed conditions, in view of the existing uncertainty concerning the phonon anharmonicity channels it seems interesting to study all possible scenarios. Moreover, even if the zone-edge process turns out to be forbidden at normal pressure, it is likely to appear at high pressures. Indeed, the measured pressure (volume) dependence of phonon frequencies<sup>29</sup> shows that the energy of the zone-center LO phonon increases with growing pressure, while the total energy of the zone-edge LO and TA phonon pair slowly decreases. The cross-over pressure and the phonon replica line shapes close to the cross-over would yield information both on the phonon energy relations and on the anharmonic coupling strength.

The paper is organized as follows: The section II introduces the model and discusses the formal quantities conveniently characterizing the system dynamics. Technical derivation is contained in the section III. The physical discussion of the result is given in the section IV. The section V concludes the paper with final remarks.

## II. THE MODEL AND THE FORMALISM

We consider the Hamiltonian describing a single exciton interacting with LO phonons,

$$H = H_X + H_{\text{ph}} + H_{\text{int}}. \quad (1)$$

The first part is the exciton Hamiltonian,

$$H_X = \sum_n \epsilon_n a_n^+ a_n,$$

where  $\epsilon_n$  is the energy of the  $n$ th exciton state and  $a_n, a_n^\dagger$  are the corresponding annihilation and creation operators. Our discussion will be simplified by using the specific structure of the excitonic spectrum in self-assembled InAs/GaAs systems<sup>4</sup>. Due to the much larger hole effective mass, the lowest excited states are formed to a good approximation by exciting the hole. Therefore, the lowest excited states of the confined exciton may be modeled by products of the corresponding harmonic oscillator

wave functions ( $\sim \exp[-(r_i/l_i)^2/2]$ ; ground state for the electron and ground or excited state for the hole), with Gaussian widths  $l_i$  given in Table I. The resulting excited two-particle states are either strictly optically inactive due to parity or almost inactive because the ground state electron and excited state hole wave functions are close to orthogonal even in absence of strict selection rules. The excitation energy typical for such inactive states is  $\sim 15$  meV, consistent with the thermally activated contribution to the central line broadening measured in experiment<sup>1</sup>. The lowest optically active state involves excitation of both the electron and the hole and its energy is typically much higher ( $\sim 70$  meV). Thus, even the LO replicas of the lowest excited state(s) lie still below the active state. Under totally non-selective excitation all states contribute to the dynamics and the resulting evolution would be both difficult to describe theoretically and hard to interpret experimentally. Therefore, we assume some degree of spectral selectivity due to finite pulse length, sufficient to avoid the excitation of the optically active excited state, and include in our description only the lowest, optically inactive excited state.

The phonon Hamiltonian  $H_{\text{ph}}$  describes the LO and TA phonon branches coupled by anharmonicity<sup>20</sup>,

$$H_{\text{ph}} = \sum_{\mathbf{k}} \Omega_{\mathbf{k}} b_{\mathbf{k}}^\dagger b_{\mathbf{k}} + \sum_{\mathbf{k}} \omega_{\mathbf{k}} c_{\mathbf{k}}^\dagger c_{\mathbf{k}} + \sum_{\mathbf{k}, \mathbf{k}'} W(\mathbf{k}, \mathbf{k}') b_{\mathbf{k}} b_{\mathbf{k}-\mathbf{k}'}^\dagger c_{\mathbf{k}'}^\dagger + \text{H.c.},$$

where  $b_{\mathbf{k}}, b_{\mathbf{k}}^\dagger$  and  $c_{\mathbf{k}}, c_{\mathbf{k}}^\dagger$  refer to LO and TA phonons with momentum  $\mathbf{k}$ , respectively, and  $\Omega_{\mathbf{k}}, \omega_{\mathbf{k}}$  are the corresponding energies. To simplify the notation, we put  $\hbar = 1$ ,  $k_B = 1$ . The anharmonic term describes a decay of LO phonon into a TA phonon and another LO phonon, which may be allowed by energy and momentum conservation only when the final states lie in the vicinity of the  $L$  point of the Brillouin zone<sup>20,24</sup>. The interaction term accounts for the Fröhlich interaction between confined charges and the lattice polarization induced by the LO deformation,

$$H_{\text{int}} = \frac{1}{\sqrt{N}} \sum_{\mathbf{k}, n, n'} F_{n, n'}(\mathbf{k}) a_n^+ a_{n'} \left( b_{\mathbf{k}} + b_{-\mathbf{k}}^\dagger \right), \quad (2)$$

where the coupling constants for the confined carriers are given by

$$F_{n, n'}(\mathbf{k}) = -\frac{e}{k} \sqrt{\frac{\hbar \Omega_0}{2v\varepsilon_0 \tilde{\varepsilon}}} \int d^3 \mathbf{r}_e d^3 \mathbf{r}_h \times \Psi_n^*(\mathbf{r}_e, \mathbf{r}_h) (e^{i\mathbf{k} \cdot \mathbf{r}_e} - e^{i\mathbf{k} \cdot \mathbf{r}_h}) \Psi_{n'}(\mathbf{r}_e, \mathbf{r}_h). \quad (3)$$

where  $\mathbf{r}_e, \mathbf{r}_h$  denote the coordinates of the electron and hole, respectively,  $\epsilon_0$  is the vacuum dielectric constant, and the other elements of the notation are described in Table I, along with values (corresponding to InAs/GaAs system) used in the calculations.

The system properties may be experimentally studied in the frequency or time domain. Although usual spectral

Effective dielectric constant <sup>30</sup>	$\tilde{\epsilon}$	62.6
Optical phonon energy <sup>24</sup>	$\hbar\Omega_0$	36 meV
Unit crystal cell volume	$v$	0.044 nm <sup>3</sup>
$\Gamma$ point LO dispersion parameter <sup>24</sup>	$\beta_{\text{LO},\Gamma}$	-0.04 meV·nm <sup>2</sup>
$L$ point LO dispersion parameters <sup>24</sup> :		
parallel to the zone boundary	$\beta_{\text{LO},\parallel}$	0.17 meV·nm <sup>2</sup>
perpendicular to the z. b.	$\beta_{\text{LO},\perp}$	0.35 meV·nm <sup>2</sup>
$L$ point TA dispersion parameters <sup>24</sup> :		
parallel to the zone boundary	$\beta_{\text{TA},\parallel}$	0.16 meV·nm <sup>2</sup>
perpendicular to the z. b.	$\beta_{\text{TA},\perp}$	-0.04 meV·nm <sup>2</sup>
Zone-center phonon lifetime <sup>20</sup>	$\tau_{\text{LO}}$	9.2 ps
Wave function widths:		
electron, in-plane	$l_{e,\perp}$	4.0 nm
hole, in-plane	$l_{h,\perp}$	3.3 nm
electron and hole, z-direction	$l_z$	1 nm

TABLE I: The parameters used in the calculations.

functions describe the equilibrium properties of the system and are relevant only in the linear response regime, in the limiting case of ultrafast excitation they are sufficient for the description of the system evolution also in the strongly driven case. This is possible due to separation of the time scales (external driving vs. phonon response): the laser pulse prepares an initial state while the subsequent evolution consists in relaxation to equilibrium.

To see this more formally, let us note that the electromagnetic wave is coupled only to carrier degrees of freedom and not to lattice modes so that all information accessible to optical measurement is given by the reduced density matrix of the carrier subsystem,

$$\varrho(t) = \text{Tr}_{\text{L}}[U(t)\rho(0)U^\dagger(t)],$$

where  $\rho(0)$  is the initial state of the total system and the trace is taken over the lattice (phonon) degrees of freedom. Assuming that the state  $n$  is the only relevant optically active state in the frequency sector of interest, the optical properties are determined by the non-diagonal element of the reduced density matrix of the carrier subsystem, proportional to the optical polarization,

$$\varrho_n(t) = \langle \text{vac} | \varrho(t) | n \rangle = \text{Tr} [\rho(0) a_n(t)], \quad (4)$$

where  $|\text{vac}\rangle$  stands for vacuum (empty dot). Let us consider a change in the carrier subsystem performed by the ultrafast pulse that takes the initial vacuum state instantaneously into a certain superposition of the vacuum state and the single-exciton state  $n$ , i.e.,  $|\psi\rangle = \cos \frac{\alpha}{2} |\text{vac}\rangle + \sin \frac{\alpha}{2} a_n^\dagger |\text{vac}\rangle$ , where  $\alpha$  is the area of the ultrafast driving pulse. Due to its inertia, the lattice is left in its initial state, i.e. in thermal equilibrium described by the density matrix  $\rho_{\text{L}}$ . The further dynamics, after switching off the pulse, is generated by the Hamiltonian (1), conserving the number of excitons. Inserting the ini-

tial state  $\rho(0) = |\psi\rangle\langle\psi| \otimes \rho_{\text{L}}$  into Eq. (4) one gets

$$\varrho_n = \frac{1}{2} \sin \alpha I_n(t),$$

where the exciton correlation function is defined by

$$I_n(t) = \langle a_n(t) a_n^\dagger(0) \rangle \quad (5)$$

( $\langle \cdot \rangle$  denotes the thermal average). Thus, the arbitrary angle  $\alpha$  factors out and the evolution is described universally by a single function  $I(t)$ .

The function (5) corresponds to the “survival amplitude”, i.e., to the overlap between the state of an exciton created instantaneously at  $t = 0$  and evolving under the full carrier-phonon Hamiltonian until the time  $t$  and the unperturbed exciton state. For our discussion it is essential that this correlation function is related to the standard Green functions formalism. Indeed, defining the retarded Green function

$$G_{nn'}(\omega) = \int dt e^{i\omega t} \Theta(t) \langle \{a_n(t), a_{n'}^\dagger\} \rangle$$

and the corresponding spectral density

$$A_n(\omega) = -2\text{Im}G_{nn}(\omega), \quad (6)$$

one can write<sup>31</sup>

$$\begin{aligned} A_n(\omega) &= \left(1 - e^{-\omega/T}\right)^{-1} \int_{-\infty}^{\infty} I_n(t) e^{i\omega t} dt \quad (7) \\ &\simeq \int_{-\infty}^{\infty} I_n(t) e^{i\omega t} dt. \end{aligned}$$

The final approximation is justified by the fact that for a typical semiconductor, the exciton energy is 1–2 orders of magnitude larger than the thermal energy even at room temperature, so the Boltzmann factor in this formula may be neglected. The experimentally measurable absorption is proportional to  $A_n(\omega)$ . Hence, both the linear spectrum and the evolution after a (possibly strong) ultrashort pulse is conveniently described within the Green function approach.

### III. EXCITON GREEN FUNCTION

In order to find the diagonal Green function  $G_{nn}(\omega)$  we write the Dyson equation in the Matsubara formalism,

$$G_{nm}(ip_\nu) = G_{nm}^{(0)}(ip_\nu) + G_{nl}^{(0)}(ip_\nu) \Sigma_{ll'}(ip_\nu) G_{l'm}(ip_\nu).$$

In order to approximately invert this system of equations we note that the diagonal Green functions are of zeroth order in the carrier-phonon interaction while the non-diagonal ones, as well as the the mass operator elements  $\Sigma_{nn'}$ , are at least of the second order. Hence, the system may be inverted to the leading order to yield the diagonal exciton Green function

$$G_n(ip_\nu) \equiv G_{nn}(ip_\nu) = \frac{1}{ip_\nu - \epsilon_n - \Sigma_n(ip_\nu)},$$

where  $\Sigma_n(ip_\nu) \equiv \Sigma_{nn}(ip_\nu)$ .

Throughout the paper, the Greek indices will be used for numbering Matsubara frequencies, while the Latin ones for exciton states (including all the relevant quantum numbers). In the single-exciton approximation, the exciton may be treated as a fermion, with the corresponding frequencies  $p_\nu$ . The bosonic frequencies are denoted by  $\omega_\mu$ , while  $\epsilon_n$  denotes the bare exciton energy in the eigenstate  $n$ .

The corresponding retarded functions are

$$\begin{aligned} G_n(\omega) &= G_n(ip_\nu)|_{ip_\nu \rightarrow \omega + i\delta} \\ \Sigma_n(\omega) &= \Sigma_n(ip_\nu)|_{ip_\nu \rightarrow \omega + i\delta}. \end{aligned}$$

Writing the retarded mass operator as  $\Sigma_n(\omega) = \Delta_n(\omega) - i\gamma_n(\omega)$ , one has

$$G_n(\omega) = \frac{1}{\omega - \epsilon_n - \Delta_n(\omega) + i\gamma_n(\omega) + i\delta}. \quad (8)$$

The energy levels  $E_n$  for the exciton interacting with LO phonons (the confined excitonic polaron<sup>4,32</sup>) may be found as the poles of this function; their real parts are given by the equation

$$E_n - \epsilon_n - \Delta_n(E_n) = 0. \quad (9)$$

Let us note that the correction  $\Delta_n(\omega)$  in the denominator of Eq. (8) is important only near  $\epsilon_n$ , where the other term vanishes (otherwise, it is a higher-order correction). Therefore, it may be replaced by

$$\Delta_n(\omega) \approx \Delta_n(E_n) + (\omega - E_n) \left( \frac{d\Delta_n(\omega)}{d\omega} \right)_{\omega=E_n}$$

and combined with  $\epsilon_n$  to give  $E_n$ , in accordance with Eq. (9).

Thus, one may write

$$G_n(\omega) = Z_n^{-1} \frac{1}{\omega - E_n + i\gamma_n(\omega)}, \quad (10)$$

where

$$Z_n = 1 - \frac{d\Delta_n(\omega)}{d\omega}|_{\omega=E_n}. \quad (11)$$

Restricting the discussion to the weak coupling case, we are interested in the single-phonon approximation, except for including the lowest-order anharmonicity effects into the LO phonon propagation. Therefore, we neglect the vertex correction in the mass operator  $\Sigma_n(ip_\nu)$  and replace the exact phonon Green function by the free one perturbed by the coupling to TA phonons in the leading order. The mass operator in this approximation is given by

$$\Sigma_n(ip_\nu) = -\frac{1}{\beta} \frac{1}{N} \sum_{n',\mathbf{k}} \sum_{\mu} |F_{nn'}(\mathbf{k})|^2 G_{n'}(ip_\nu - i\omega_\mu) D(\mathbf{k}, i\omega_\mu), \quad (12)$$

and the LO phonon Green function is

$$D(\mathbf{k}, i\omega_\mu) = -\frac{2\Omega_\mathbf{k}}{-(i\omega_\mu)^2 + \Omega_\mathbf{k}^2 + 2\Omega_\mathbf{k}\Pi(\mathbf{k}, i\omega_\mu)}. \quad (13)$$

The polarization operator in the proposed approximation involves the lowest order anharmonicity correction

$$\Pi(\mathbf{k}, i\omega_\mu) = -\frac{1}{\beta} \frac{1}{N} \sum_{\mathbf{k}',\mu'} |W(\mathbf{k}, \mathbf{k}')|^2 D_{\text{LO}}^{(0)}(\mathbf{k} - \mathbf{k}', i\omega_\mu - i\omega_{\mu'}) D_{\text{TA}}^{(0)}(\mathbf{k}', i\omega_{\mu'}). \quad (14)$$

Inserting the free phonon Green functions into Eq. (14) and performing the summation over frequencies one gets

$$\begin{aligned} \Pi(\mathbf{k}, i\omega_\mu) &= \\ &- \frac{2}{N} \sum_{\mathbf{k}'} |W(\mathbf{k}, \mathbf{k}')|^2 \left[ \frac{(n_{\mathbf{k}'} - N_{\mathbf{k}-\mathbf{k}'}) (\Omega_{\mathbf{k}-\mathbf{k}'} - \omega_{\mathbf{k}'})}{(i\omega_\mu)^2 - (\Omega_{\mathbf{k}-\mathbf{k}'} - \omega_{\mathbf{k}'})^2} + \frac{(n_{\mathbf{k}'} + N_{\mathbf{k}-\mathbf{k}'} + 1) (\Omega_{\mathbf{k}-\mathbf{k}'} + \omega_{\mathbf{k}'})}{(i\omega_\mu)^2 - (\Omega_{\mathbf{k}-\mathbf{k}'} + \omega_{\mathbf{k}'})^2} \right], \end{aligned} \quad (15)$$

where  $N_{\mathbf{k}}$  and  $n_{\mathbf{k}}$  are the Bose distributions for LO and TA phonons, respectively, with momentum  $\mathbf{k}$ .

The Green functions may be written in the representation

$$D(\mathbf{k}, i\omega_\mu) = \int_{-\infty}^{\infty} \frac{d\omega}{2\pi} \frac{B(\mathbf{k}, \omega')}{i\omega_\mu - \omega'}, \quad G_{n'}(i\omega_\mu) = \int_{-\infty}^{\infty} \frac{d\omega}{2\pi} \frac{A_{n'}(\omega')}{i\omega_\mu - \omega'}, \quad (16)$$

where the phonon spectral density is defined as

$$B(\mathbf{k}, \omega') = -2\text{Im}D(\mathbf{k}, \omega'). \quad (17)$$

The frequency summation in Eq. (12) may now be performed, leading to

$$\Sigma_n(ip_\nu) = -\frac{1}{N} \sum_{n',\mathbf{k}} |F_{nn'}(\mathbf{k})|^2 \int_{-\infty}^{\infty} \frac{d\omega'}{2\pi} \int_{-\infty}^{\infty} \frac{d\omega''}{2\pi} [n_{\text{B}}(\omega') + 1] \frac{B(\mathbf{k}, \omega') A_{n'}(\omega'')}{\omega' + \omega'' - ip_\nu}.$$

From the above, using Eq. (16), the retarded mass operator reads

$$\Sigma_n(\omega) = -\frac{1}{N} \sum_{n',\mathbf{k}} |F_{nn'}(\mathbf{k})|^2 \int_{-\infty}^{\infty} \frac{d\omega'}{2\pi} [n_B(\omega') + 1] B(\mathbf{k}, \omega') G_{n'}(\omega - \omega'), \quad (18)$$

and, inserting Eq. (10),

$$\Delta_n(\omega) = -\frac{1}{N} \sum_{n',\mathbf{k}} |F_{nn'}(\mathbf{k})|^2 \int_{-\infty}^{\infty} \frac{d\omega'}{2\pi} [n_B(\omega') + 1] B(\mathbf{k}, \omega') \frac{\omega - \omega' - E_{n'}}{(\omega - \omega' - E_{n'})^2 + \gamma_n^2(\omega - \omega')}, \quad (19a)$$

$$\gamma_n(\omega) = \frac{1}{N} \sum_{n',\mathbf{k}} |F_{nn'}(\mathbf{k})|^2 \int_{-\infty}^{\infty} \frac{d\omega'}{2\pi} [n_B(\omega') + 1] B(\mathbf{k}, \omega') \frac{\gamma_n(\omega - \omega')}{(\omega - \omega' - E_n)^2 + \gamma_n^2(\omega - \omega')}. \quad (19b)$$

To the leading order,  $\Delta_n(\omega)$  and  $\gamma_n(\omega)$  may be obtained from Eq. (19a,b) by setting  $\gamma_n(\omega) \rightarrow 0$  on the right-hand side, which leads to

$$\Delta_n(\omega) = -\frac{1}{N} \sum_{n',\mathbf{k}} |F_{nn'}(\mathbf{k})|^2 \int_{-\infty}^{\infty} \frac{d\omega'}{2\pi} [n_B(\omega) + 1] \frac{B(\mathbf{k}, \omega')}{\omega - \omega' - E_{n'}}, \quad (20a)$$

$$\gamma_n(\omega) = \frac{1}{2N} \sum_{n',\mathbf{k}} |F_{nn'}(\mathbf{k})|^2 B(\mathbf{k}, \omega - E_{n'}) [n_B(\omega - E_{n'}) + 1]. \quad (20b)$$

According to Eqs. (17) and (13), the phonon spectral density is given by

$$B(\mathbf{k}, \omega) = \frac{8\Omega_{\mathbf{k}}^2 \text{Im} \Pi(\mathbf{k}, \omega)}{[\omega^2 - \Omega_{\mathbf{k}}^2 + 2\Omega_{\mathbf{k}} \text{Re} \Pi(\mathbf{k}, \omega)]^2 + [2\Omega_{\mathbf{k}} \text{Im} \Pi(\mathbf{k}, \omega)]^2}. \quad (21)$$

The essential contribution to  $\Delta_n(\omega)$  may be obtained by setting  $\Pi(\mathbf{k}, \omega) \rightarrow 0$  in Eq. (21); after a simple integration one gets

$$\Delta_n(\omega) = \frac{1}{N} \sum_{\mathbf{k}, n'} |F_{nn'}(\mathbf{k})|^2 \left[ \frac{1 + N_{\mathbf{k}}}{\omega - E_{n'} - \Omega_{\mathbf{k}}} + \frac{N_{\mathbf{k}}}{\omega - E_{n'} + \Omega_{\mathbf{k}}} \right].$$

Hence, from Eq. (11),

$$Z_n = 1 + \frac{1}{N} \sum_{\mathbf{k}, n'} |F_{nn'}(\mathbf{k})|^2 \left[ \frac{1 + N_{\mathbf{k}}}{(E_n - E_{n'} - \Omega_{\mathbf{k}})^2} + \frac{N_{\mathbf{k}}}{(E_n - \omega - E_{n'} + \Omega_{\mathbf{k}})^2} \right]. \quad (22)$$

To find  $\gamma_n(\omega)$  we get the retarded polarization operator  $\Pi(\mathbf{k}, \omega)$  from Eq. (15) by  $i\omega_{\mu} \rightarrow \omega + i\delta$ ; thus

$$\begin{aligned} \chi(\mathbf{k}, \omega) &\equiv \text{Im} \Pi(\mathbf{k}, \omega) \\ &= \frac{\pi}{N} \sum_{\mathbf{k}'} |W(\mathbf{k}, \mathbf{k}')|^2 \{ (n_{\mathbf{k}'} - N_{\mathbf{k}-\mathbf{k}'}) [\delta(\omega - \Omega_{\mathbf{k}-\mathbf{k}'} + \omega_{\mathbf{k}'}) - \delta(\omega + \Omega_{\mathbf{k}-\mathbf{k}'} - \omega_{\mathbf{k}'})] \\ &\quad + (n_{\mathbf{k}'} + N_{\mathbf{k}-\mathbf{k}'} + 1) [\delta(\omega - \Omega_{\mathbf{k}-\mathbf{k}'} - \omega_{\mathbf{k}'}) - \delta(\omega + \Omega_{\mathbf{k}-\mathbf{k}'} + \omega_{\mathbf{k}'})] \}. \end{aligned} \quad (23)$$

According to Eq. (21), the contribution from LO phonons to the spectral density  $B(\mathbf{k}, \omega - E_{n'})$  in Eq. (20b) is peaked around  $\omega - E_{n'} \approx \pm \Omega_{\mathbf{k}}$ . Hence, the Bose function takes the values of  $n_B(\Omega_{\mathbf{k}}) + 1$  and  $n_B(-\Omega_{\mathbf{k}}) + 1 = -n_B(\Omega_{\mathbf{k}})$ . If we assume that the temperature is well below 400 K, the former is close to one and the latter is zero. Thus,  $\omega \approx E_{n'} + \Omega_{\mathbf{k}}$  and we may approximate, neglecting the LO phonon energy shift due to anharmonic

coupling,

$$\begin{aligned} \gamma_n(\omega) &= \\ &\frac{1}{N} \sum_{n',\mathbf{k}} |F_{nn'}(\mathbf{k})|^2 \frac{\chi(\mathbf{k}, \omega - E_{n'})}{[\omega - E_{n'} - \Omega_{\mathbf{k}}]^2 + \chi^2(\mathbf{k}, \omega - E_{n'})}. \end{aligned} \quad (24)$$

There are a few effects contained in this formula. First, it generates a broadening of the zero-phonon spectral peak at  $\omega = E_n$  due to LO phonon-assisted transitions. In the absence of anharmonic coupling ( $\chi \rightarrow 0$ )

an energy conserving Dirac  $\delta$  appears on the right-hand side, restricting the process to exact resonance. The anharmonicity releases this restriction and leads to two-phonon anharmonicity-induced processes whenever the energy spacing matches an LO+LA or LO+TA pair, as described in detail in Ref. 15,26. Further broadening comes from the usual second-order two-phonon processes which are beyond the leading-order approximation used here. For the ground state, however, all these processes are of phonon absorption type and are negligible at low temperatures. The second effect, which is of major interest to us in the present work, is related to the line shape of the LO phonon replica (around  $\omega \approx E_{n'} + \Omega_{\mathbf{k}}$ ) and its effect on the system evolution.

In this spectral region only the first and third terms from Eq. (23) contribute to Eq. (24) since the energies of LO phonons lie entirely above the TA branch. Out of these two, the first one vanishes at low temperatures. Moreover, since coupling to short-wavelength modes is favored both by the general form of the coupling ( $\sim \sqrt{k'}$ , see Ref. 33) and by the growing density of states, this contribution (for low  $k$ , as selected by the exciton-LO-phonon form factor<sup>4,15</sup>) is peaked around  $\omega - E_{n'} \approx 20$  meV (for GaAs, see Ref. 24 for exact dispersion curves) and gives smaller contribution due to large denominator in Eq. (24). The remaining term corresponds to the LO phonon decay with emission of another LO phonon and TA phonon. It is large, when the total energy of the resulting phonons is close to the  $\Gamma$ -point LO phonon energy, i.e. near the  $L$  point in the Brillouin zone<sup>20,24</sup>. Thus, we approximate the coupling constant and the Bose distribution by the corresponding  $L$ -point values, assuming also  $\mathbf{k}$  near the zone center. Replacing the summation by integration we obtain, after these approximations,

$$\chi(\mathbf{k}, \omega) = \frac{v\pi}{(2\pi)^3} |W(0, \mathbf{k}_L)|^2 (n_{\mathbf{k}_L} + 1) \times \int d^3 k' \delta(\omega - \Omega_{\mathbf{k}-\mathbf{k}'} - \omega_{\mathbf{k}'}),$$

where  $v$  is the unit cell volume. The problem is thus reduced to finding the appropriate two-phonon density of states. We assume that LO and TA phonon energies may be approximated by quadratic forms of momenta around each  $L$  point, given by the matrices  $\hat{\beta}_{\text{LO}}^{(i)}$  and  $\hat{\beta}_{\text{TA}}^{(i)}$ , respectively. The index  $i = 1 \dots 4$  numbers the four pairs of opposite hexagonal walls of the Brillouin zone (note that the four tensors differ only by orientation). Near the  $i$ th  $L$  point, the minimum total energy of a LO+TA pair with total momentum  $\mathbf{k}$  is

$$\xi_{\mathbf{k}}^{(i)} = \omega_{\mathbf{k}_L} + \Omega_{\mathbf{k}_L} + \mathbf{k} \hat{\beta}_{\text{LO}}^{(i)} (\hat{\beta}^{(i)})^{-1} \hat{\beta}_{\text{LO}}^{(i)} \mathbf{k},$$

where  $\hat{\beta}^{(i)} = \hat{\beta}_{\text{LO}}^{(i)} + \hat{\beta}_{\text{LA}}^{(i)}$ . It is clear that the LO phonon with momentum  $\mathbf{k}$  may decay via this process only if  $\Omega_{\mathbf{k}} > \xi_{\mathbf{k}} \equiv \min_i \xi_{\mathbf{k}}^{(i)}$ . One finds,

$$\int d^3 k' \delta(\omega - \Omega_{\mathbf{k}-\mathbf{k}'} - \omega_{\mathbf{k}'}) = \sum_i \int_{S'_i} \frac{dS'}{2|\hat{\beta}^{(i)} \mathbf{k}'|}$$

where the surface  $S'_i$  in the  $\mathbf{k}'$  space, composed by all states satisfying energy and momentum conservation, is defined by  $\xi_{\mathbf{k}}^{(i)} + \mathbf{k} \hat{\beta}^{(i)} \mathbf{k} = \omega$  (the integral is zero if this equation has no solutions, i.e. for  $\omega \leq \xi_{\mathbf{k}}^{(i)}$ ). Thus, the finite bandwidth of phonon branches leads to a (lower) frequency cutoff in the two-phonon density of final states for the anharmonic process.

For GaAs, the tensors  $\hat{\beta}^{(i)}$  may be reasonably approximated isotropically (and hence become equal). Defining  $\beta = (\det \hat{\beta}^{(i)})^{1/3}$ , one finds explicitly

$$\chi(\mathbf{k}, \omega) = \sum_i \chi^{(i)}(\mathbf{k}, \omega),$$

where

$$\chi^{(i)}(\mathbf{k}, \omega) = \frac{v}{4\pi} |W(0, \mathbf{k}_L)|^2 (n_{\mathbf{k}_L} + 1) \beta^{-3/2} \sqrt{\omega - \xi_{\mathbf{k}}^{(i)}}$$

for  $\omega \geq \xi_{\mathbf{k}}^{(i)}$  and  $\chi^{(i)}(\mathbf{k}, \omega) = 0$  otherwise. Since, most probably, the zone-edge LO+TA process is only one of many LO phonon damping mechanisms, we shall phenomenologically add to  $\chi(\mathbf{k}, \omega)$  an additional contribution  $\chi_0$ , corresponding to all the other damping processes.

As discussed above,  $\gamma_n(\omega)$  contains various contributions, related to the broadened zero-phonon line, LO phonon replica, and acoustic phonon sidebands<sup>2</sup> (not included in our discussion). As long as these features are spectrally separated, as is the case for the ground exciton state at low temperatures, they manifest themselves by processes on different timescales (1 ns exponential decay<sup>1,34</sup>, 1 ps overdamped acoustic phonon dynamics<sup>2</sup>, 100 fs LO phonon beats damped on 10 ps timescale as discussed below). These processes may, therefore, be experimentally separated even if they are superposed on one another. As we are mostly interested in the LO phonon features we simply model the low-frequency sector by a Lorentzian, allowing for a certain broadening of the zero-phonon line. Separating this low-frequency part from the peak around  $\omega = E_0 + \Omega_{\mathbf{k}}$ , we write the spectral density for the ground exciton state in the form

$$A_0(\omega) = 2Z_0^{-1} \frac{\gamma_0}{(\omega - E_0)^2 + \gamma_0^2} + \frac{2}{N} \sum_{n', \mathbf{k}} \Phi_{nn'}(\mathbf{k}) g_{\mathbf{k}}(\omega - \Omega_{\mathbf{k}} - E_{n'}), \quad (25)$$

where

$$\Phi_{nn'}(\mathbf{k}) = \frac{|F_{nn'}(\mathbf{k})|^2}{(E_{n'} - E_n + \Omega_{\mathbf{k}})^2}, \quad (26)$$

$$g_{\mathbf{k}}(\omega) = \frac{\chi(\mathbf{k}, \omega + \Omega_{\mathbf{k}})}{\omega^2 + \chi^2(\mathbf{k}, \omega + \Omega_{\mathbf{k}})}, \quad (27)$$

and  $\gamma_0$  accounts for the broadening of the zero-phonon line. The first contribution corresponds to the central peak while the second part describes the exciton dressing with a continuum of LO phonon modes.

#### IV. THE TIME EVOLUTION: DAMPED LO PHONON BEATS

The time-dependent correlation function for  $t > 0$ , derived from Eq. (25) according to Eq. (7), is

$$I_0(t) = Z_0^{-1} e^{-i(E_0 - i\chi_0)t} + \frac{1}{N} \sum_{n',\mathbf{k}} \Phi_{0n'}(\mathbf{k}) g_{\mathbf{k}}(t) e^{-i(E_{n'} + \Omega_{\mathbf{k}})t}, \quad (28)$$

where

$$g_{\mathbf{k}}(t) = \int \frac{d\omega}{\pi} g_{\mathbf{k}}(\omega) e^{-i\omega t} \equiv |g_{\mathbf{k}}(t)| e^{i\varphi_{\mathbf{k}}(t)}. \quad (29)$$

Using Eq. (22) in the low temperature limit ( $N_{\mathbf{k}} \rightarrow 0$ ), one gets

$$|I_0(t)|^2 = \left( 1 - 2 \frac{1}{N} \sum_{n,\mathbf{k}} \Phi_{0n}(\mathbf{k}) \right) + 2 \frac{1}{N} \sum_{n,\mathbf{k}} \Phi_{0n}(\mathbf{k}) |g_{\mathbf{k}}(t)| \cos [(E_0 - E_n - \Omega_{\mathbf{k}})t + \varphi_{\mathbf{k}}(t)]. \quad (30)$$

Hence, the evolution of each LO phonon mode in the polarization cloud may be treated separately. The total effect emerges as a superposition of such individual contributions, weighted by the coupling strengths. It should be noted that in spite of the growing energy separation in the denominator of the coupling strength (26) (for  $n = 0$ ), the coupling to higher levels ( $n' \geq 1$ ) is stronger than that to the  $n' = 0$  level because of the charge cancellation which reduces the diagonal coupling constants  $F_{00}(\mathbf{k})^4$ .

Let us study a few examples of the system evolution. The numerical results presented below have been obtained with the GaAs parameters shown in Tab. I. The anharmonic coupling strength  $|W(0, \mathbf{k}_L)|$  was determined from the requirement that the zone-edge LO+TA decay process should be responsible for 90% of the experimentally known decay probability of the  $\Gamma$ -point LO phonon. A specific LO mode  $\mathbf{k}$  is damped by the zone-edge process if  $\chi(\mathbf{k}, \Omega_{\mathbf{k}}) > 0$ , i.e. if its energy lies over the density of states (DOS) cutoff,  $\Omega_{\mathbf{k}} > \xi_{\mathbf{k}}$ . In our parabolic dispersion model one has

$$\Omega_{\mathbf{k}} - \xi_{\mathbf{k}} = \Omega_0 - \Omega_{\mathbf{k}_L} - \omega_{\mathbf{k}_L} + \max_i \mathbf{k} \left[ \hat{\beta}_{\Gamma} - \hat{\beta}_{\text{LO}}^{(i)} (\hat{\beta}^{(i)})^{-1} \hat{\beta}_{\text{TA}}^{(i)} \right] \mathbf{k},$$

where the last term is negative except for a very small positive contribution (sensitive to the crudeness of dispersion modeling) in a narrow solid angle around the (111) and equivalent directions (towards the  $L$  points). Hence, if the decay process is forbidden for the  $\Gamma$ -point mode it is also forbidden for a vast majority of all the modes. Two different regimes may arise when this process is allowed for a given mode:

If the decay results in states distant from the zone edge then the density of final states is also far from its edge. Quantitatively, for

$$\sqrt{\Omega_{\mathbf{k}} - \xi_{\mathbf{k}}} \gg \frac{v|W(0, \mathbf{k}_L)|^2}{2\pi\beta^{3/2}} (n_{\mathbf{k}_L} + 1),$$

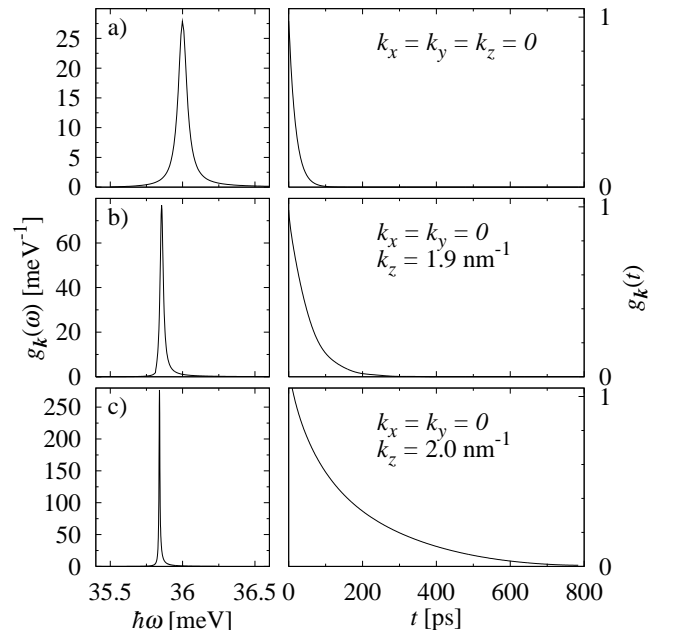


FIG. 1: Single mode line shape (left) and temporal evolution (envelope of LO oscillations, right) for three modes with wave vectors as shown, for  $\Omega_0 - \Omega_{\mathbf{k}_L} - \omega_{\mathbf{k}_L} = -0.5$  meV.

one has

$$\frac{\partial \chi(\mathbf{k}, \omega)}{\partial \omega} \Big|_{\omega=\Omega_{\mathbf{k}}} \ll 1,$$

and the value of  $\chi(\mathbf{k}, \omega)$  is almost constant around the LO phonon energy, leading to the Lorentzian line shape (for this specific mode) and exponential decay (Fig 1a). The decay time of oscillations induced by a mode in  $|I_n(t)|^2$  is twice longer than the decay time of the mode occupation (which would be governed by  $|g_{\mathbf{k}}|^2$ ). In fact, the homogeneity of the “regular” decay (far from the DOS edge) justifies representing all such decay processes by a single

constant  $\chi_0$ . On the other hand, if the anharmonic decay process leads to zone-edge states, then  $\xi_{\mathbf{k}}$  is close to  $\Omega_{\mathbf{k}}$  and the line shape is determined mostly by the frequency dependence of  $\chi(\mathbf{k}, \omega)$  and becomes non-Lorentzian (Fig. 1b).

If the mode energy lies below the DOS cutoff, the mode is damped only by the other processes, represented by  $\chi_0$  (Fig. 1c). The vicinity of the DOS edge still results in dephasing effects (by virtual processes) manifested by a non-Lorentzian line shape.

In principle, all the three scenarios may be present among modes forming the polaronic cloud, leading to intricate system dynamics. However, since it is rather impossible to excite a single, selected mode, the observable evolution always results from superposing the dynamics of all the modes forming the polaron cloud. Such dynamics (and the corresponding line shape) averages the contributions from different modes. Moreover, the joint evolution is affected by the dephasing effect resulting from dispersion<sup>2,4,19</sup>. Let us note that, according to Eqs. (25,28), several contributions may be present in the system evolution, related not only to the ground state itself but also from non-adiabatic excitation of optically inactive excited states, the latter being much more pronounced due to lack of charge cancellation. However, the excited state contributions correspond to higher frequencies and may be selectively turned off by modifying the pulse duration (i.e. its spectral width). Below we present the results assuming the excitation of the ground state only and of the ground and first excited state. We neglect the broadening of the central line which, in the time range of interest, would produce an additional weak slope in the time evolution.

Before discussing the results, let us note that in the case of a single exciton state and without any phonon anharmonicity the problem is reduced to the independent boson model which is solvable exactly<sup>2</sup>. This allows us to estimate the accuracy of our approximate approach by comparing it with the exact result in this limiting case. As shown in Fig. 2a the Green function technique gives very exact results, which is due to the fact that the overall phonon-induced perturbation is very weak.

The results of our calculations for the full case including anharmonic phonon decay processes are shown in Fig. 2b-d. We calculated the shapes of the LO replica lines for various possible energy relations at the zone edge. If the momentum and energy conservation for all effectively coupled modes (with spectral width  $\Delta\Omega_{\mathbf{k}}$ ) is satisfied by final states lying far from the zone edge, i.e. if  $\Omega_0 - \Omega_{\mathbf{k}_L} - \omega_{\mathbf{k}_L} \gg \Delta\Omega_{\mathbf{k}}$  (large energy overlap at the zone edge), the difference of decay times between modes becomes small and beats corresponding to all the modes decay with the same lifetime  $\tau$ , equal to the doubled lifetime of the bulk zone-center LO phonon  $\tau_{\text{LO}}$ . In this case, the damping dominates over dephasing. However, since the damping and dephasing times are still comparable, the dispersion-induced dephasing effect is not negligible and reduces the decay rate of the whole phonon dressing

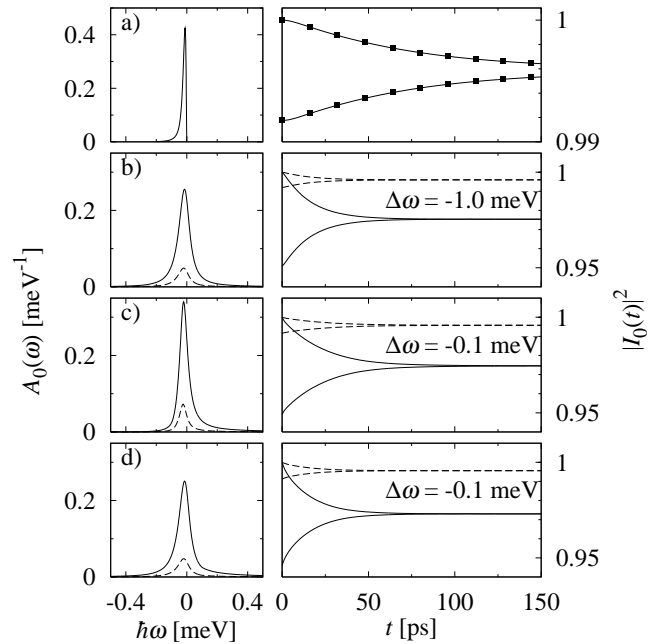


FIG. 2: (a) The hypothetical line shape of the LO phonon replica of the ground exciton state without anharmonic damping (broadened only due to dispersion) and the corresponding envelope of LO phonon beats (line) compared to the exact result (squares). (b-d) The line shapes of the phonon replicas corresponding to the ground state (dashed lines) and to the first excited optically inactive state (solid lines) and the corresponding envelope of the phonon beats for three values of the band overlap as shown. The central frequency  $\omega_0$  corresponds to  $E_n + \Omega_0$  for each line. In plots (b) and (c) it is assumed that the zone-edge process contributes 90% of the decay probability. In (d), where the zone-edge process is forbidden, the anharmonic LO-TA coupling is the same as in (c).

cloud oscillations below the individual mode rate  $2\tau_{\text{LO}}$  (Fig. 2b).

If, on the other hand, the zone-edge energy overlap is small, then some modes will be weakly affected by the zone-edge mechanism and some others will be unaffected by it. Thus, some modes off the  $\Gamma$  point live much longer than the zone-center mode and the overall decay time of the phonon beats may become longer than  $2\tau_{\text{LO}}$  (Fig. 2c).

Finally, let us consider a situation when the LO+TA process is forbidden for the zone center phonon. Although some other modes still may decay via this process, this effect is too weak to be noticeable in the overall dynamics and the phonon replica line again takes the Lorentzian shape with decay time shorter than the  $\tau_{\text{LO}}$  due to dispersion.

## V. CONCLUSIONS

In this paper we have studied the quantum evolution of the exciton-LO-phonon system in an InAs/GaAs quantum dot, focusing on the possible signature of the zone-edge LO $\rightarrow$ LO+TA anharmonic decay in the line shapes of the LO phonon replicas and in the time evolution of the system. Apart from including anharmonic damping, we have further extended the description by incorporating contributions from optically inactive excited states. We have shown that the vicinity of the edge of density of final states leads to the appearance of long-living modes and to a deviation from the symmetric Lorentzian line shape. In such case, the decay time of the LO phonon beats becomes longer than  $2\tau_{\text{LO}}$ , where  $\tau_{\text{LO}}$  is the measured decay time of the zone-center LO phonon population. This situation appears when the total energy of the  $L$ -point phonons (LO+TA) is only slightly lower (by  $\sim 0.1$  meV) than the  $\Gamma$ -point LO phonon energy. On the other hand, when this energy overlap becomes larger, the line shape becomes very close to Lorentzian and the decay time of the LO phonon beats is shorter than  $2\tau_{\text{LO}}$ , due to additional contribution from dispersion-induced dephasing.

In view of long coherence time of the undamped LO phonon oscillations (due to weak dispersion), the line shapes of the phonon replicas and the time evolution of beats is always determined by the anharmonic damping processes. Therefore, the damping effect must be included in any description of carrier-LO-phonon dynamics. Moreover, in some special cases, the detailed structure of phonon bands may noticeably influence the measurable properties. It may therefore be possible to extract information about the anharmonic LO phonon damping channels from the QD spectroscopy data. Al-

though the phonon dispersion is obviously a material characteristics, it may be modified by changing the material composition and experimental conditions (e.g. pressure), so a range of dynamical regimes might be observed.

It may be expected that an actual experiment will be performed on the ensemble of dots by nonlinear optical techniques, e.g. four-wave-mixing (FWM). It is known that the time-resolved FWM results cannot be reproduced exactly by a linear spectrum or by a single pulse dynamics<sup>3</sup>. Unlike for the Markovian dephasing effects, in the case of the lattice response related to pure dephasing after a fast excitation there is no simple relation between the spectra and time-resolved evolutions obtained in linear and nonlinear experiments. However much similarity still remains, due to the unique underlying physical effects. For instance, the variation of damping times and the non-Lorentzian shape of the LO replica reflect the structure of the allowed final states for an anharmonic decay process and may be expected to appear in any kind of experiment. Hence, the results obtained here are at least qualitatively relevant also for a nonlinear experiment, although an exact extension in this direction would certainly be desirable. Another important generalization should consist in including final-length pulses<sup>5,35,36</sup>.

## Acknowledgments

This paper has been supported by the Polish Ministry of Scientific Research and Information Technology under the (solicited) grant No PBZ-Min-008/P03/03 and by the Polish KBN under grant No. PB 2 PO3B 085 25. P.M. is grateful to the Alexander von Humboldt Foundation for generous support.

---

<sup>1</sup> P. Borri, W. Langbein, S. Schneider, U. Woggon, R. L. Sellin, D. Ouyang, and D. Bimberg, Phys. Rev. Lett. **87**, 157401 (2001); Phys. Rev. B **66**, 081306 (2002).

<sup>2</sup> B. Krummheuer, V. M. Axt, and T. Kuhn, Phys. Rev. B **65**, 195313 (2002).

<sup>3</sup> A. Vagov, V. M. Axt, and T. Kuhn, Phys. Rev. B **66**, 165312 (2002); **67**, 115338 (2003).

<sup>4</sup> L. Jacak, P. Machnikowski, J. Krasnyj, and P. Zoller, Eur. Phys. J. D **22**, 319 (2003).

<sup>5</sup> R. Alicki, M. Horodecki, P. Horodecki, R. Horodecki, L. Jacak, and P. Machnikowski, Phys. Rev. A **70**, 010501 (2004), quant-ph/0302058.

<sup>6</sup> P. Machnikowski and L. Jacak, Phys. Rev. B **69**, 193302 (2004), cond-mat/0305165.

<sup>7</sup> G. C. Cho, W. Kütt, and H. Kurz, Phys. Rev. Lett. **65**, 764 (1990).

<sup>8</sup> L. Bányai, D. B. Tran Thoai, E. Reitsamer, H. Haug, D. Steinbach, M. U. Wehner, M. Wegener, T. Marschner, and W. Stolz, Phys. Rev. Lett. **75**, 2188 (1995).

<sup>9</sup> M. U. Wehner, M. H. Ulm, D. S. Chemla, and M. Wegener, Phys. Rev. Lett. **80**, 1992 (1998).

<sup>10</sup> C. Fürst, A. Leitenstorfer, A. Laubereau, and R. Zimmermann, Phys. Rev. Lett. **78**, 3733 (1997).

<sup>11</sup> M. U. Wehner, D. S. Chemla, and M. Wegener, Phys. Rev. B **58**, 3590 (1998).

<sup>12</sup> P. Roussignol, D. Ricard, C. Flytzanis, and N. Neuroth, Phys. Rev. Lett. **62**, 312 (1989).

<sup>13</sup> R. W. Schoenlein, D. M. Mittleman, J. J. Shiang, A. P. Alivisatos, and C. V. Shank, Phys. Rev. Lett. **70**, 1014 (1993).

<sup>14</sup> D. M. Mittleman, R. W. Schoenlein, J. J. Shiang, V. L. Colvin, A. P. Alivisatos, and C. V. Shank, Phys. Rev. B **49**, 14435 (1994).

<sup>15</sup> L. Jacak, J. Krasnyj, D. Jacak, and P. Machnikowski, Phys. Rev. B **67**, 035303 (2003).

<sup>16</sup> D. Steinbach, G. Kocherscheidt, M. U. Wehner, H. Kalt, M. Wegener, K. Ohkawa, D. Hommel, and V. M. Axt, Phys. Rev. B **60**, 12079 (1999).

<sup>17</sup> V. M. Axt, M. Herbst, and T. Kuhn, Superlattices and Microstructures **26**, 118 (1999).

<sup>18</sup> L. Besombes, K. Kheng, L. Marsal, and H. Mariette, Phys. Rev. B **63**, 155307 (2001).

<sup>19</sup> E. Pazy, *Semicond. Sci. Technol.* **17**, 1172 (2002).

<sup>20</sup> F. Vallée and F. Bogani, *Phys. Rev. B* **43**, 12049 (1991).

<sup>21</sup> S. Barman and G. P. Srivastava, *Appl. Phys. Lett.* **81**, 3395 (2002).

<sup>22</sup> A. R. Bhatt, K. W. Kim, and M. A. Stroscio, *J. Appl. Phys.* **76**, 3905 (1994).

<sup>23</sup> X.-Q. Li and Y. Arakawa, *Phys. Rev. B* **57**, 12285 (1998).

<sup>24</sup> D. Strauch and B. Dorner, *J. Phys.: Cond. Matt.* **2**, 1457 (1990).

<sup>25</sup> O. Verzelen, R. Ferreira, and G. Bastard, *Phys. Rev. B* **62**, R4809 (2000).

<sup>26</sup> L. Jacak, J. Krasnyj, D. Jacak, and P. Machnikowski, *Phys. Rev. B* **65**, 113305 (2002).

<sup>27</sup> O. Verzelen, G. Bastard, and R. Ferreira, *Phys. Rev. B* **66**, 081308 (2002).

<sup>28</sup> V. M. Fomin, V. N. Gladilin, S. N. Klimin, J. T. Devreese, P. M. Koenraad, and J. H. Wolter, *Phys. Rev. B* **61**, R2436 (2000).

<sup>29</sup> R. Trommer, H. Müller, M. Cardona, and P. Vogl, *Phys. Rev. B* **21**, 4869 (1980).

<sup>30</sup> S. Adachi, *J. Appl. Phys.* **58**, R1 (1985).

<sup>31</sup> G. D. Mahan, *Many-Particle Physics* (Kluwer, New York, 2000).

<sup>32</sup> O. Verzelen, R. Ferreira, and G. Bastard, *Phys. Rev. Lett.* **88**, 146803 (2002).

<sup>33</sup> E. M. Lifshitz and L. P. Pitaevskii, *Physical Kinetics* (Butterworth-Heinemann, Oxford, 1997).

<sup>34</sup> M. Bayer and A. Forchel, *Phys. Rev. B* **65**, 041308 (2002).

<sup>35</sup> H. Castella and R. Zimmermann, *Phys. Rev. B* **59**, R7801 (1999).

<sup>36</sup> P. Machnikowski and L. Jacak, *Semicond. Sci. Technol.* **19**, S299 (2004), cond-mat/0307615.